Detection of distortions in images of natural scenes in mild traumatic brain injury patients

Jennings BJ[1,2], Schmidtmann G[2,4], Wehbé F[2], Kingdom FAA[2] and Farivar R[2,3].

[1]Centre for Cognitive Neuroscience, Department of Psychology, College of Health and Life Sciences, Brunel University, London, UK.

[2]McGill Vision Research Unit, Department of Ophthalmology, McGill University, Montreal, Canada

[3]Traumatic Brain Injury Program, Research Institute of the McGill University Health Centre, Montreal, Canada

[4]Eye & Vision Research Group, Department of Optometry, University of Plymouth, Plymouth, UK.

Keywords: Mild traumatic brain injury (mTBI), natural scenes, spatial distortions.

Abstract

Mild traumatic brain injuries (mTBI) frequently lead to the impairment of visual functions including blurred and/or distorted vision, due to the disruption of visual cortical mechanisms. Previous mTBI studies have focused on specific aspects of visual processing, e.g., stereopsis, using artificial, low-level, stimuli (e.g., Gaussian patches and gratings). In the current study we investigated high-level visual processing by employing images of real world natural scenes as our stimuli. Both an mTBI group and control group composed of healthy observers were tasked with detecting sinusoidal distortions added to the natural scene stimuli as a function of the distorting sinusoid's spatial frequency. It was found that the mTBI group were equally as sensitive to high frequency distortions as the control group, however sensitivity decreased more rapidly with decreasing distortion frequency in the mTBI group relative to the controls. These data reflect a deficit in the mTBI group to spatially integrate over larger regions of the scene.

Introduction

A mild traumatic brain injury (mTBI) is a head injury resulting from a blunt trauma or sudden positive or negative acceleration that causes the brain to abruptly translate and impact with the rigid internal surface of the skull. Additionally, due to differences in the densities of white and grey matter a relative motion, e.g., shearing/stretching, can occur away from the impact location at the gray-white matter interface resulting in a diffuse axonal injury being sustained (Ghajari, Hellyer & Sharp, 2017). Excessive strain can also be sustained by the corpus callosum as the two hemi-sphere composing the brain shear relative to each other potentially leading to axonal injury (Bigler & Maxwell, 2012).

Up to 5.3 million people are affected by TBI every year in the USA (Coronado, Xu, Basavaraju, & McGuire, 2011; Corrigan, Selassie, & Orman, 2010; Langlois, Rutland-Brown, & Wald, 2006), leading to hospitalization and disability (Greenwald, Kapoor, & Singh, 2012; Kapoor & Ciuffreda, 2002). In the year 1999 in Ontario (Canada) approximately 100 per 100,000 males (<19 years of age) sustained a traumatic brain injury, the rate for females was approximately half that of males (Walker et al., 2001). According to the *National Center for Injury Prevention and Control* (2003) approximately 75% of all TBIs are classified as mild (mTBI). mTBI is diagnosed if at least one of the following symptoms is observed immediately following injury; (i) confusion/disorientation, (ii) impaired consciousness/memory dysfunction occurring at the time of injury, and (iii) a loss of consciousness of a duration less than 30 minutes. While these symptoms are termed mild, significant cognitive, e.g., memory (Flynn, 2010) and visual impairments can persist following the injury. TBI-associated visual deficits are diverse and include blurred/distorted vision, double vision, reading problems, reduced global stereopsis, increased sensitivity to motion and flicker, and eye strain (Capó-Aponte, Urosevich, Temme, Tarbett, & Sanghera, 2012; Ciuffreda et al., 2008; Greenwald et al., 2012; Kapoor & Ciuffreda, 2002; Schmidtmann *et al*., 2017; Spiegel, Laguë-Beauvais, Sharma, & Farivar, 2015). For a complete review of potential visual specific deficits see the comprehensive review of Armstrong (2018).

Previous studies have suggested that TBI results in the disruption and dysfunction of long-distance cortical connections (Spiegel, Laguë-Beauvais, Sharma, & Farivar, 2015; see Hulkower, Poliak, Rosenbaum, Zimmerman, & Lipton, 2013; Sharp, Scott, & Leech, 2014 for recent reviews), caused by axonal shearing (Inglese et al., 2005). This raises the question of whether mTBI affects the spatial integration of visual information. The aim of this study is to address this question, by measuring the sensitivity to artificial spatial distortions, of varying spatial frequency, applied to images of natural scenes.

Previously, Kingdom, Olmos & Field (2007) investigated sensitivity for detecting a variety of transformations (‘distortions’) applied to images of natural scenes. They found that observers were least sensitive to those transformations that are commonly encountered in the natural world, for example, a horizontal translation or a rotation. It was concluded that the visual system achieves this invariance to spatial transformations at least partially via a process in which information is discarded. Recently, Jennings *et al*. (2015) investigated sensitivity for detecting a particularly unnatural spatial distortion, not commonly encountered in real world natural vision; a vertical and horizontal sinusoidal distortion. It was demonstrated that when this distortion was applied to an image of a natural scene, sensitivity (for detection) increased as the spatial frequency of the distortion increased, i.e. higher frequency distortions are more salient (see Figure 1 for a demonstration). Interestingly, it was shown that sensitivity was identical, independent of whether the undistorted comparison scene was of the same scene or an entirely different image. Hence, distortion detection thresholds are equal if a distorted scene *A* is compared to the undistorted comparison image of scene *A*, or a different undistorted image, scene *B* (within a single trial of a 2-alternative forced choice paradigm). This was the case over the whole range of distortion frequencies tested. Jennings *et al*. (2015) concluded that a in-build mechanism, probably acquired via previous exposure to the real world, must exist that signals to observers how an undistorted real world scene should appear. This interpretation is consistent with a previous conclusion drawn by Bex (2010). It is this mechanism that can be relied upon to make distortion detections when identical undistorted comparison scene is unavailable.

The current study addresses the question of whether this real-world appearance mechanism is disrupted after a mTBI has been sustained, possibly as a result of any injury induced, cortically based, distorted/blurry vision. Any visual disruption could manifest itself via higher distortion detection thresholds being measured when the *test* (i.e., a distorted scene) and *comparison* (i.e., an undistorted scene) are different within a single trial. On the other hand, it could be that case simply that higher thresholds are measured for all conditions with the mTBI population, as potentially their internally distorted vision could mask the physical distortions present in the stimuli.

General Methods

Observers

Two groups of observers were recruited for the study. The control group consisted of 15 observers (10 females, age: 23.7±5.2 (mean±SD)). The clinical group consisted of a sample of 15 participants (9 females, age: 43.1±15.8 (mean±SD)) with a history of mTBI, recruited via the McGill University Health Centre Out-Patient TBI Program.

The criteria for the mTBI diagnosis were: (i) any amnesia of events immediately before or after the accident lasting no longer than 24 hours, and (ii) a Glasgow Coma Score ranging between 13 and 15. A loss of consciousness was sustained at the time of injury that persisted for <30 minutes.

All procedures were in accordance with the Code of Ethics of the World Medical Association (Declaration of Helsinki) and were approved by the Research Ethics Board of the McGill University Health Centre. Informed consent was obtained from all participants prior to data collection.

Neuropsychological and optometric pre-screening

All participants underwent a variety of neuropsychological screening, which included: (i) a visual attention tests (Trail Making Test A and B (Giovagnoli et al., 1996) and Bells Test (Gauthier, Dehaut, & Joanette, 1989) and (ii), a spatial neglect test utilizing the Clock-drawing test (Ishiai, Sugishita, Ichikawa, Gono, & Watabiki, 1993). In addition, a short verbal screening for relevant medical history was conducted, included questions regarding recurrent migraines, psychiatric disorders, or vertigo. The exclusion criteria were general anaesthesia within the past six months, other acquired brain injuries in the past, severe tremors and/or epilepsy, double vision and manifest strabism. In order to minimize the contribution of any optometric and oculomotor-related visual impairments, the observers were also tested for the presence of a strabismus (Cover-Uncover and Alternating Cover Tests), where the magnitude of heterophoria was measured with the Maddox Rod Test. Furthermore, monocular and binocular visual acuity was tested at a viewing distance of 4 m (Logarithmic Visual Acuity Chart; Precision Vision, Lasalle, IL, USA). The ocular dominance was determined by using the Miles Test. Additionally, the observers completed a questionnaire adapted from *Assessment and Management of Visual Dysfunction Associated with Mild Traumatic Brain Injury for the Defense Centers of Excellence for Psychological Health and Traumatic Brain Injury* (Spiegel et al., 2016).

Equipment

A PC running Windows 7, with MatLab (MathWorks Inc) installed with the Psychtoolbox (Brainard, 1997; Pelli, 1997; Kleiner, Brainard, Pelli 2007). The stimuli display device was CRT running at 60 Hz with a resolution of 1600 x 1200 pixels. During testing observers' heads were stabilized with a chin and forehead rest, this also maintained a constant viewing distance of 50 cm. All observer responses were made via a numeric keypad.

Stimuli, psychophysical task and data processing

All stimuli were generated using images of natural scenes selected from the McGill Calibrated Images Database (Olmos & Kingdom, 2004). A subset of images were selected from the database, examples of which are depicted in figure. 1, the scenes varied in type (e.g., natural landscapes, urban scenes, etc), scale (e.g., zoomed in/out) and time of year represented (e.g., winter, etc).

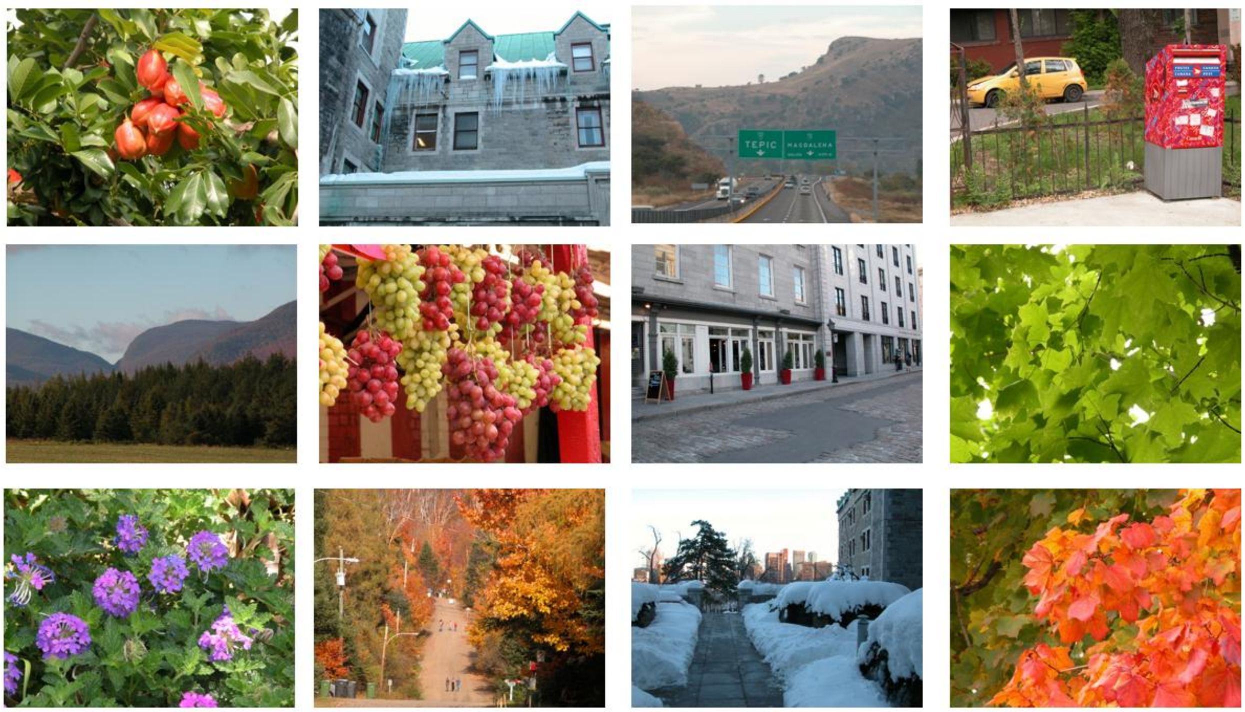

Figure 1 Examples of the raw natural images employed to produce the experimental stimuli.

From the raw image database a stimuli database with predefined distortion levels was created (during testing a staircase procedure selected the distortion amplitude for the succeeding trail and appropriate stimuli were retrieved from the image database). For each of the three distortion frequencies tests stimuli with a range of amplitudes were generated. First, square (600 x 600 pixels) subsections were pseudo-randomly selected and gamma corrected from the raw images. Second, a horizontal and vertical sinusoidal distortion was applied at the required spatial frequency and amplitude level.

Thirdly, a soft circular Gaussian edge was applied in order to blend the edge of the scene images into the wider mid-grey background covering the remainder of the display. All presented scenes subtended 15.3° of visual angle and during testing observers did not see the same scene more than once. Physical measurements were made from the display device while an image of a regular grid distorted at different frequencies was displayed. The measurement of the peak-to-peak distance in these images (i.e., distance between maximum compression locations) allowed calibration of the input distortion coefficient, via a linear fitted function, transforming it into a value defined by cycles per degree.

The six tested conditions consisted of three *same* conditions, i.e., within each trial the test (distorted) and comparison (undistorted) scenes were identical. The other three conditions were the *different* conditions, i.e., where within each trial the *test* (distorted) and *comparison* (undistorted) intervals composing one trial contained different scenes. For both the same and different conditions three distortion frequencies were tested, they were; 0.065, 0.262 and 0.524 cycles/deg. Examples of distorted scenes at four different distortion amplitudes (this independent variable) as a function of distortion frequency are shown in Figure 2; distortion amplitudes vary along the ordinate (rendered at suprathreshold levels for illustration purposes), as a function of the three distortion frequencies shown on the abscissa.

Figure 2 A plot showing the effect of increasing the applied distortion's amplitude to an image of a natural scene as a function of distortion spatial frequency.

Figure 3 illustrates the time-course of one trial of each of the *same* (a) and *different* (b) conditions. The same scene is employed in both intervals of the *same* conditions, with one (chosen at random) containing the distortion. While, in the *different* condition, different scenes are employed within a single trial; again one being chosen at random to contain the distortion. The temporal properties of each condition were identical. In each interval both scenes were displayed for 500 ms, separated by a 500 ms interstimulus-interval, after the second interval the screen displayed a mid-grey, which remained until the observer submitted their response, this initiated the start of the next trial. Throughout each testing block observers were instructed to maintain fixation on the central white cross.

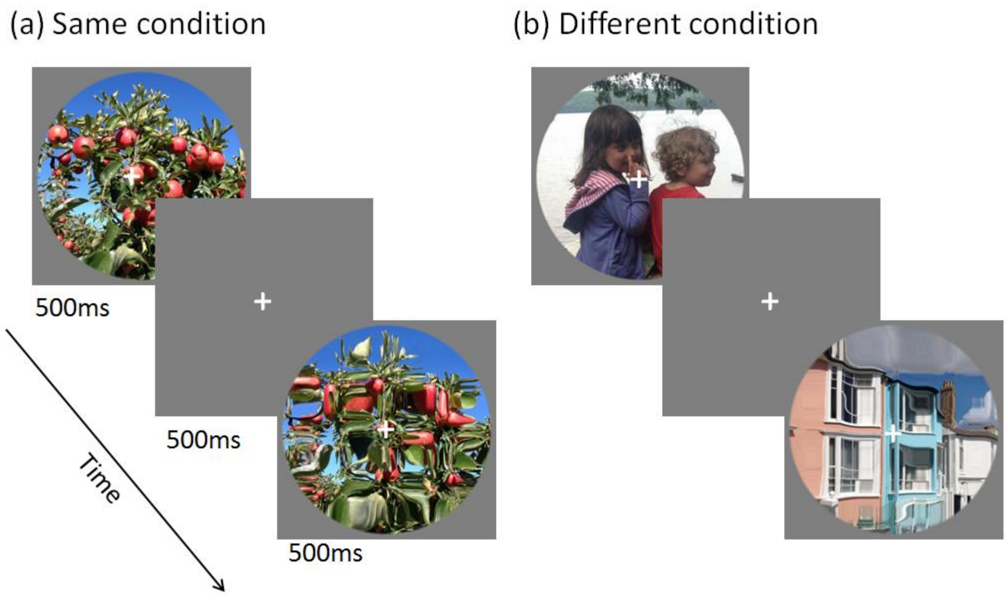

Figure 3a-b The time course of each trial is indicated for (a) the same and (b) the different conditions.

Distortion detection thresholds, i.e., the magnitude (amplitude) of the distorting sinusoid, were obtained via an adaptable staircase. The number of correct responses was extracted from the raw staircase data for each tested condition level prior to having a psychometric function (logistic) fitted. Thresholds were subsequently estimated by determining the amplitude that corresponded to a proportion correct of 0.75. All fitting was realised by employing functions from the Palamedes toolbox (Prins & Kingdom, 2009).

Results

Distortion detection thresholds

Mean distortion detection thresholds are plotted as a function of distortion frequency in Figure 4a-b, the TBI data is plotted in magenta, while the control group is plotted in blue. All t-tests reported in are 2-tailed and p-values are reported after an appropriate Bonferroni adjustment for multiple comparisons was applied. Significant differences exist between the TBI and control group for the lowest distortion frequency tested for both the same and different presentation conditions (same condition: $t(29)=6.40$, $p<.001$, different condition: $t(29)=6.03$, $p>.001$), the corresponding effect sizes for these conditions were found, according to the common magnitude descriptors (Cohen, 1988; Sawilowsky, 2009), to both be ‘huge’ (same: 2.30 and different: 2.17). All other conditions were found to be insignificant (as indicated ‘ns’ in Figure 4a and b), all ps>.44.

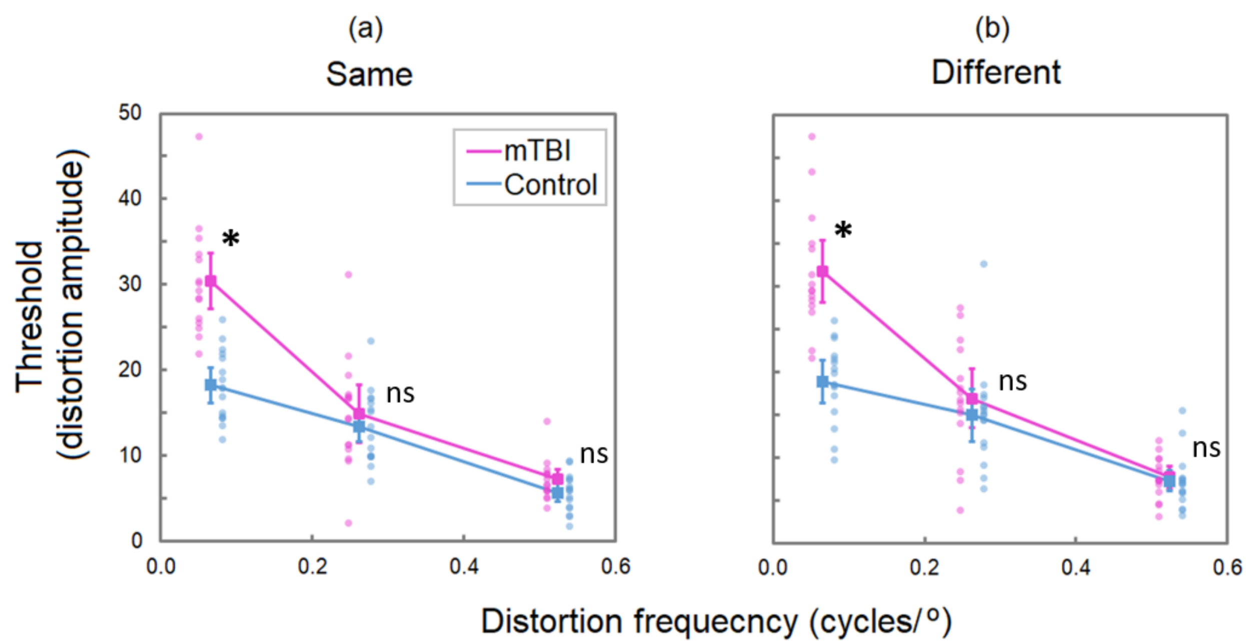

Figure 4a-b Plot showing the variation of distortion detection thresholds as a function of distortion frequency for both the same (a) and different (b) conditions. The magenta plots the mTBI data, while the control group is plotted in blue. The solid squares indicate the mean values, the small circles represent individual observer thresholds and the error bars represent ±2 standard errors.

Correlation of performance with age in the mTBI group

The data presented in the current study is consistent with the TBI group suffering from a deficit in spatial integration processing relative to the control group. It has previously been reported that older observers show a reduced performance in spatial integration tasks (Andersen & Ni, 2008; Del Viva & Agostini, 2007). Additionally, a significant difference in age existed between the TBI and control group ($t(29)=-4.61$, $p<.001$). Even though the mTBI group in the current study were significantly younger than the older observers used in aging studies (i.e., >70 years) individual thresholds and ages were analyzed to determine if any significant correlations exist, this could provide evidence that the observed decline performance within the mTBI group can simply be explained as an aging effect.

Individual thresholds for each of the six tested conditions (3 distortions frequencies x 2 presentation conditions (*same* and *different*)) were correlated with observer age. The results are plotted in Figure 5a and b (same and different conditions, respectively), the green, blue and grey points correspond to distortions frequencies of 0.065, 0.262 and 0.524 cycles/°. No significant relationships were revealed within any of the six conditions, i.e., thresholds cannot be predicted from age. All Pearson correlation coefficients were within the range: $-0.26 \leq r \leq 0.36$, while all corresponding p-values were insignificant and within the range: $0.19 \leq p \leq .58$.

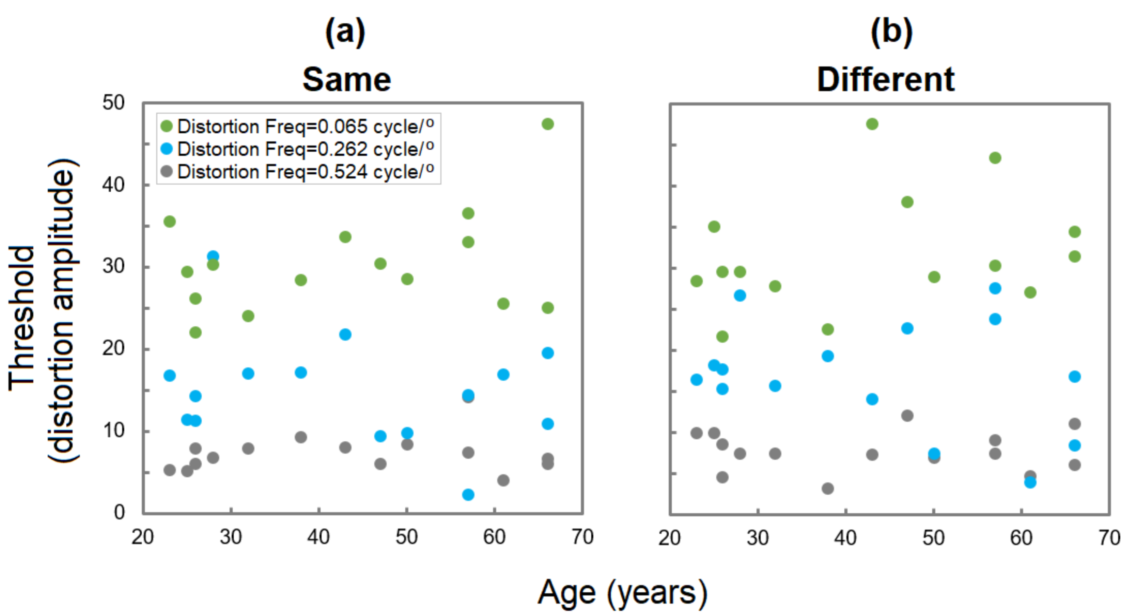

***Figure 5a-b** Each measured threshold is plotted as a function of age for the same and different conditions (panels a and b, respectively) for the three distortion frequencies tested, these are*

coded as blue, red and green points, corresponding to distortions frequencies of 0.065, 0.262 and 0.524 cycles/°. No significant relationships exist.

Correlation of performance with VA in the mTBI group

In order to determine whether the measured effect is sensory in nature rather than a consequence of optometric deficits, we performed correlation analyses between the measured (binocular) visual acuity and distortion thresholds obtained in the mTBI group. Any significant correlations would provide evidence that the decline performance is potentially due to an optical defect.

The results are plotted in Figure 6a and b (same and different conditions, respectively), the green, blue and grey points correspond to distortions frequencies of 0.065, 0.262 and 0.524 cycles/°. No significant relationships were revealed within any of the six conditions, i.e., thresholds cannot be predicted based on visual acuity. All Pearson correlation coefficients were within the range: $-0.40 \leq r \leq 0.37$, while all corresponding p-values were insignificant and within the range: $0.14 \leq p \leq 1$.

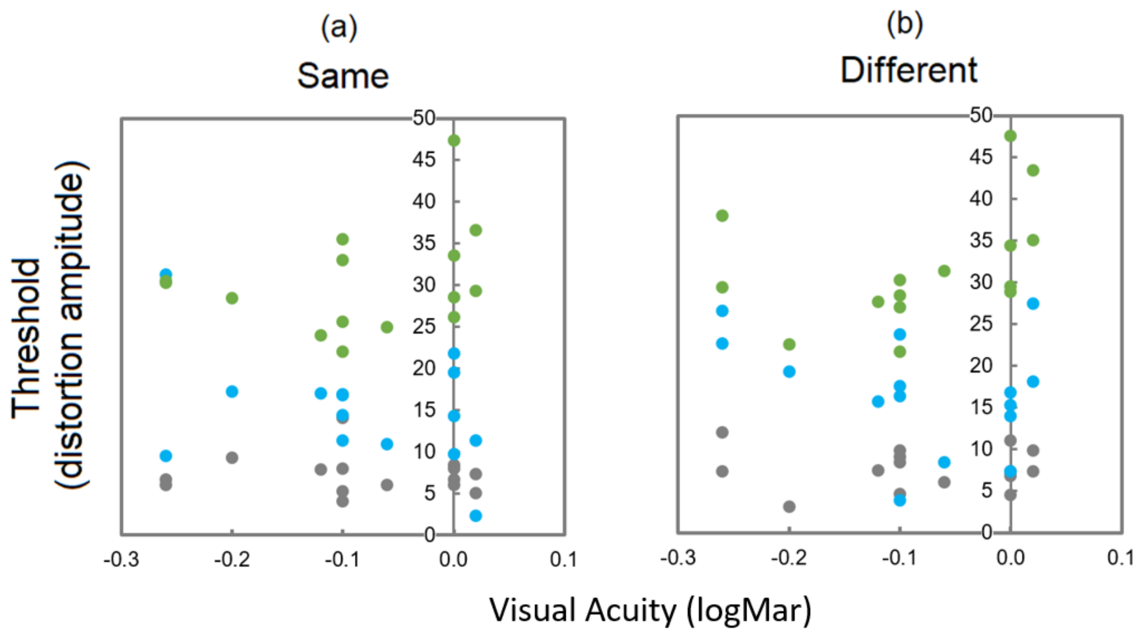

Figure 6a-b Each measured threshold is plotted as a function of age for the same and different conditions (panels a and b, respectively) for the three distortion frequencies tested, these are coded as blue, red and green points, corresponding to distortions frequencies of 0.065, 0.262 and 0.524 cycles/°. No significant relationships exist.

Discussion

The main findings of the study are summarised;

(i) Both the control and mTBI group showed a greater sensitivity (lower thresholds) for detecting high frequency distortions, consistent with Jennings *et al*. (2015).

(ii) No differences were found (within the control and mTBI groups) between the *same* and *different* conditions, i.e., comparing control-to-control or mTBI-to-mTBI between Figure 4a, consistent with Jennings *et al*. (2015).

(iii) Thresholds were found to be significantly elevated in the mTBI group relative to the control group only for the lowest distortion frequency tested (on *both* the same and *different* conditions).

(iv) No correlation exists between age and the measured detection thresholds in the mTBI group, this excludes the data being explained as an aging effect.

(iv) No correlation exists between visual acuity and the measured detection thresholds in the mTBI group, this excludes the data being explained as an aging effect.

The results presented in this paper indicate that the mTBI patients show similar sensitivity as normal observers for detecting higher frequency distortions present in images of natural scenes, but exhibit reduced sensitivity for detecting low frequency distortions, i.e., they have difficulty spatially integrating over larger regions of a scene.

The lack of reduction in sensitivity for the high frequency condition in the mTBI group perhaps suggests that the mTBI are not suffering from a visual deficit similar to traditional blurred vision, i.e., similar in appearance to blur produced by within-eye refractive errors, as for example resulting from myopia. If this was the case measured detection thresholds would have been expected to be been elevated for the high frequency condition, as mechanism inducing the blur would have filtered out the high frequency distortion information.

As sensitivity is equal for both the same and different conditions, i.e., sensitivity is equal independent of whether an identical undistorted comparison scene is presented, the mTBI group appears to have an intact internal mechanism signaling to them how the structure of the real world should appear.

This deficiency in spatial integration of visual information could be due to axonal shearing. A potential explanation being that the mTBI resulted in axonal shearing which in turn led to a disruption of long-distance cortical connections.

Acknowledgments

This research was funded by the Psychological Health and Traumatic Brain Injury Research Program of the U.S. Department of Defense under award W81XWH-14-1-0320. Views and opinions of, and endorsements by the author(s) do not reflect those of the US Army or the Department of Defense.

Priority interest statement

There are no known conflicts of interest associated with this publication and there has been no significant financial support for this work that could have influenced its outcome.

References

Andersen GJ, Ni R. (2008). Aging and visual processing: declines in spatial not temporal integration. Visual Psychophysics and Physiological Optics. 48(1):109-18.

Armstrong, R. A. (2018). Visual problems associated with traumatic brain injury: Vision with traumatic brain injury. DOI: 10.1111/cxo.12670.

Bex, P. J. (2010). (In) Sensitivity to spatial distortion in natural scenes. Journal of Vision, 10(2):23, 1–15.

Bigler ED, Maxwell WL. (2012). Neuropathology of mild traumatic brain injury: relationship to neuroimaging findings. Brain Imaging Behav. 6(2):108-36.

Brainard, D. H. (1997). The Psychophysics Toolbox. Spatial Vision, 10(4), 433–436.

Capó-Aponte, J. E., Urosevich, T. G., Temme, L. A., Tarbett, A. K., & Sanghera, N. K. (2012). Visual dysfunctions and symptoms during the subacute stage of blast-induced mild traumatic brain injury. Military Medicine, 177(7), 804–813.

Ciuffreda, K. J., Rutner, D., Kapoor, N., Suchoff, I. B., Craig, S., & Han, M. E. (2008). Vision therapy for oculomotor dysfunctions in acquired brain injury: a retrospective analysis. Optometry, 79(1), 18–22.

Cohen, J. (1988). Statistical Power Analysis for the Behavioral Sciences. Routledge. ISBN 1-134-74270-3.

Coronado, V. G., Xu, L., Basavaraju, S. V., & McGuire, L. C. (2011). Surveillance for Traumatic Brain Injury--Related Deaths --- United States, 1997--2007.

Corrigan, J. D., Selassie, A. W., & Orman, J. A. L. (2010). The Epidemiology of Traumatic Brain Injury. The Journal of Head Trauma Rehabilitation, 25(2), 72–80.

Flynn FG. Memory impairment after mild traumatic brain injury. Continuum (Minneap Minn). 2010;16(6 Traumatic Brain Injury):79–109. pmid:22810715.

Gauthier L, Dehaut F, Joanette Y. The Bells Test: a quantitative and qualitative test for visual neglect. Int J Clin Neuropsychol. 1989; 11: 49–54.

Gauthier, L., Dehaut, F., & Joanette, Y. (1989). The Bells Test: A quantitative and qualitative test for visual neglect. International Journal of Clinical Neuropsychology, 11(2), 49–54.

Ghajari, M., Hellyer, P. J., & Sharp, D. J. (2017). Computational modelling of traumatic brain injury predicts the location of chronic traumatic encephalopathy pathology. Brain, 140(2), 333–343. http://doi.org/10.1093/brain/aww317.

Giovagnoli AR, Del Pesce M, Mascheroni S, Simoncelli M, Laiacona M, Capitani E. Trail making test: normative values from 287 normal adult controls. Ital J Neurol Sci. 1996; 17: 305–309.

Giovagnoli, A. R., Del Pesce, M., Mascheroni, S., Simoncelli, M., Laiacona, M., & Capitani, E. (1996). Trail making test: normative values from 287 normal adult controls. Italian Journal of Neurological Sciences, 17(4), 305–309.

Greenwald, B. D., Kapoor, N., & Singh, A. D. (2012). Visual impairments in the first year after traumatic brain injury. Brain Injury, 26(11), 1338–1359.

Hulkower, M. B., Poliak, D. B., Rosenbaum, S. B., Zimmerman, M. E., & Lipton, M. L. (2013). A Decade of DTI in Traumatic Brain Injury: 10 Years and 100 Articles Later. AJNR. American Journal of Neuroradiology, 34(11), 2064–2074. http://doi.org/10.3174/ajnr.A3395

Inglese, M., Makani, S., Johnson, G., Cohen, B. A., Silver, J. A., Gonen, O., & Grossman, R. I. (2005). Diffuse axonal injury in mild traumatic brain injury: a diffusion tensor imaging study. Journal of Neurosurgery, 103(2), 298–303. http://doi.org/10.3171/jns.2005.103.2.0298

Ishiai S, Sugishita M, Ichikawa T, Gono S, Watabiki S. (1993). Clock-drawing test and unilateral spatial neglect. Neurology. 43:106–110.

Jennings, B. J., Wang, K, Menzies, S. & Kingdom, F. A. A. (2015). Detection of chromatic and luminance distortions in natural scenes. Journal of the Optical Society of America A, 32(9): 1613-1622.

Kapoor, N., & Ciuffreda, K. J. (2002). Vision disturbances following traumatic brain injury. Current Treatment Options in Neurology, 4(4), 271–280.

Kingdom, F. A. A., Field, D. J. & Olmos, A. (2007) Does spatial invariance result from insensitivity to change? Journal of Vision, 7(14):11, 1-13.

Kleiner M, Brainard D, Pelli D. (2007) What's new in Psychtoolbox-3? Perception. 36 ECVP Abstract Supplement.

Langlois, J. A., Rutland-Brown, W., & Wald, M. M. (2006). The Epidemiology and Impact of Traumatic Brain Injury. The Journal of Head Trauma Rehabilitation, 21(5), 375–378. http://doi.org/10.1097/00001199-200609000-00001

Maria Michela Del Viva; Rachele Agostini, R. (2007) Visual Spatial Integration in the Elderly. Investigative Ophthalmology & Visual Science, 48:2940-2946. doi:10.1167/iovs.06-0729

National Center for Injury Prevention and Control. (2003). Report to Congress on Mild Traumatic Brain Injury in the United States: Steps to Prevent a Serious Public Health Problem. Atlanta, GA: Centers for Disease Control and Prevention. Neuropathology of mild traumatic brain injury: relationship to neuroimaging findings.

Olmos, A & F. A. A. Kingdom (2004). A biologically inspired algorithm for the recovery of shading and reflectance images. Perception 33, 1463–1473.

Pelli, D. G. (1997). The VideoToolbox software for visual psychophysics: Transforming numbers into movies. Spatial Vision, 10(4), 437–442.

Prins, N., & Kingdom, F.A.A., 2009. Palamedes: Matlab routines for analyzing psychophysical data. www.palamedestoolbox.org.

Sawilowsky, S. (2009). New effect size rules of thumb. Journal of Modern Applied Statistical Methods, 8(2), 467–474.

Schmidtmann, G., Ruiz, T., Reynaud, A., Spiegel, D.P., Laguë-Beauvais, M., Hess, F.R., Farivar, R., (2017). Sensitivity to binocular disparity is reduced by mild traumatic brain injury. Invest Oph- thalmol Vis Sci. 2017; 58:2630–2635.

Sharp, D. J., Scott, G., & Leech, R. (2014). Network dysfunction after traumatic brain injury. Nature Reviews. Neurology, 10(3), 156–166.

Spiegel, D. P., Laguë-Beauvais, M., Sharma, G., & Farivar, R. (2015). Inter-hemispheric wave propagation failures in traumatic brain injury are indicative of callosal damage. Vision Research, 109(Pt A), 38–44. http://doi.org/10.1016/j.visres.2015.02.020

Spiegel, D. P., Reynaud, A., Ruiz, T., Laguë-Beauvais, M., Hess, R., & Farivar, R. (2016). First- and second-order contrast sensitivity functions reveal disrupted visual processing following mild traumatic brain injury. Vision Research, 122, 43–50.